Inorg. Chem. **2004**, *43*, 5501–5504

Synthesis, Structure, and Bonding of the Nonclassical Zintl Phase $K_5As_3Pb_3$

Michael T. Klem and John D. Corbett*

Department of Chemistry and Ames Laboratory—DOE,[1] Iowa State University, Ames, Iowa 50011

Received March 25, 2004

The title phase was synthesized by direct fusion of a stoichiometric amount of the elements followed by annealing at 650 °C for 3 weeks. The compound crystallizes in the orthorhombic space group *Pnma* (No. 62), $Z = 4$, with $a = 19.451(6)$ Å, $b = 12.164(3)$ Å, $c = 6.581(1)$ Å. The compound is made up of $As_3Pb_3^{5-}$ crown clusters that can be likened geometrically and electronically to 6-atom *hypho*-clusters derived from a tricapped trigonal prismatic *closo* parent. These crowns are interconnected via intercluster Pb–Pb bonds to form infinite chains along the *b* axis, which means the compound contains an extra two cations and two electrons per formula unit. Extended Hückel calculations indicate that the two additional electrons per cluster are accommodated in π^* states on the cluster and predict that the phase should be semiconducting. The latter is confirmed by microwave resistivity measurements, $\rho_{298} = 1.0 \times 10^2\ \mu\Omega\cdot$cm; $(\delta\rho/\delta T)/\rho = -0.14(3)\ K^{-1}$.

Introduction

Large deltahedral clusters of the tetrel elements (Tt = Si–Pb) in the neat solid state have been fairly limited. Among the largest clusters currently are the *nido*-Tt_9^{4-} anions which are now known for all of the group 14 elements except carbon.[2] An important factor limiting the stability of large deltahedral clusters of the heavy tetrel elements seems to be disproportionate size-to-charge ratio. Wade's rules for counting electron states indicate that the charge assigned to a deltahedral cluster should be independent of its nuclearity and, therefore, that large tetrel clusters should carry relatively small charges, −2 for the closo examples.[3,4] This can conceptually set up situations in which the number of cations may be insufficient to separate the large clusters, presuming that such clusters would undergo condensation or disproportionation on contact. Large organic ligands such as in the cryptated alkali-metal cations have been used in the past to achieve effective separation of such clusters,[5] whereas partial substitution of electron-poorer elements such as Cd or In serves to increase cluster charge, e.g., in K_6CdPb_8 and K_5InPb_8.[6] Alternatively, one would presumably reduce the overall charge for a typical electron-poor cluster through substitution of an electron-richer element (e.g., a pnictogen) that would contribute more electrons to the skeletal bonding of the cluster. However, this approach might instead provide a route to new heteroatomic clusters of the tetrel elements should the substitution lead to new cluster alternatives rather than just excessively low charges on normal cluster anions.

The diverse heteropolyatomic anions containing both group 14 and 15 elements that have been reported evidently all exhibit classical bonding and can be classified as Zintl phases. The 14/15 heteroatomic members in neat systems include the numerous A_5TtPn_3 (A = Li, Na; Tt = Si, Ge, Sn; Pn = P, As, Sb) with rings or chains constructed of the tetrahedra sharing either one edge or two vertices,[7] tetrahedral anions in K_8SnSb_4, six-membered rings in chains K_3SnSb_3,[8]

* Author to whom correspondence should be addressed. E-mail: jcorbett@iastate.edu.

(1) This research was supported by the Office of the Basic Energy Sciences, Materials Sciences Division, U.S. Department of Energy (DOE). The Ames Laboratory is operated for DOE by Iowa State University under Contract No. W-7405-Eng-82.

(2) (a) Queneau, V.; Sevov, S. C. *Angew. Chem.* **1997**, *109*, 1818. (b) von Schnering, H.-G.; Baitinger, M.; Bolle, U.; Cabrera, W. C.; Curda, J.; Grin, Y.; Heinemann, L.; Llanos, L.; Peters, K.; Schmeding, A.; Somer, M. *Z. Anorg. Allg. Chem.* **1997**, *623*, 1037. (c) Queneau, V.; Sevov, S. C. *Inorg. Chem.* **1998**, *37*, 1358. (d) Todorov, E.; Sevov, S. C. *Inorg. Chem.* **1998**, *37*, 3889. (e) Queneau, V.; Todorov, E.; Sevov, S. C. *J. Am. Chem. Soc.* **1998**, *120*, 3263. (f) Goichoechea, J.; Sevov, S. C. *J. Am. Chem. Soc.*, in press.

(3) Wade, K. *Adv. Inorg. Chem. Radiochem.* **1976**, *18*, 1.

(4) Sevov, S. C.; Corbett, J. D. *Z. Phys. D* **1993**, *26*, 64.

(5) Corbett, J. D. *Chem. Rev.* **1985**, *85*, 383.

(6) (a) Todorov, E.; Sevov, S. C. *Angew. Chem., Int. Ed.* **1999**, *38*, 1775. (b) Klem, M. T.; Corbett, J. D. Unpublished results.

(7) (a) Juza, R.; Schulz W. *Z. Anorg. Allg. Chem.* **1954**, *275*, 65. (b) Eisenmann, B.; Somer, M. *Z. Naturforsch., B: Chem. Sci.* **1985**, *40B*, 886. (c) Eisenmann, B.; Klein, J.; Somer, M. *Z. Kristallogr.* **1991**, *197*, 265, 267, 269. (d) Eisenmann, B.; Rossler, U. *Z. Kristallogr.—New Cryst. Struct.* **2000**, *215*, 347.

(8) Asbrand, M.; Eisenmann, B. *Z. Anorg. Allg. Chem.* **1997**, *623*, 561.

10.1021/ic040045r CCC: $27.50
Published on Web 08/04/2004

and many other examples with more condensation.[9] The mixed members in condensed systems are now extended to include evidently the first example with nonclassical bonding, the unconventional electron-rich $K_5As_3Pb_3$ in which crown-shaped As_3Pb_3 clusters are interconnected into 1-D chains. Heretofore, nonclassical bonding has been encountered most often in more electron-deficient cluster systems, particularly with triel (group 13) members.[10,11]

Experimental Section

Synthesis. The materials and general reaction techniques in welded tantalum tubes have been described elsewhere.[12,13] All transfers were completed in a N_2- or He-filled glovebox. The compound $K_5As_3Pb_3$ can be obtained by allowing stoichiometric amounts of potassium (Strem, 99.9995%), arsenic (Aesar, 99.99%), and lead (Aesar, 99.9999%) to react briefly at 900 °C in a sealed Ta container, after which the product is annealed for 3 weeks at 650 °C. (Nb tubes frequently failed under these conditions.) The result was brittle, black, and modestly air sensitive, changing color in about one minute when brought from the glovebox into the air; under less forcing conditions, broad lines of Pb might appear in some powder patterns. The latter has proven to be a good indication of the quality of the sample protection and of the sensitivity of nominally anionic lead therein to oxidation by traces of the atmosphere at room temperature. Initially, single crystals were isolated from an As-limited reaction mixture that had been loaded as K_5AsPb_8. Reactions later loaded on-stoichiometry typically yielded 80−90% of the title phase with the remainder identified by powder pattern as a combination of Pb and KPb, implying some small unseen losses of As.

X-ray Diffraction. Powder diffraction data from an Enraf-Nonius 552 Guinier camera and Cu $K\alpha_1$ radiation were used for phase identification. An improved method of sample mounting for powder pattern measurements was employed relative to cellophane tape. The powders were held between sheets of aluminized polyester film by means of a thin centered film of vacuum grease that also served to seal the outer edge of the sheets and to thereby hinder decomposition of the air sensitive products. The films were then first compared semiquantitatively with patterns calculated for phases with known structures. The distributions of products were then estimated visually from relative powder pattern intensities considering the symmetry and contents of the unit cells as well.

Several black crystals of $K_5As_3Pb_3$ were isolated, inserted into thin-walled capillaries, and checked by means of Laue photographs. Diffraction data were then collected from one at room temperature with the aid of a Rigaku AFC6R diffractometer and monochromated Mo Kα radiation. Routine indexing of 25 centered reflections gave a primitive orthorhombic cell. Systematic extinctions led to the unique assignment of space group *Pnma*. The space group assignment was confirmed by a refinement carried out with the aid of the TEXSAN package.[14] The data were corrected for absorption empirically according to three ψ-scans of strong reflections with different 2θ values. The final residuals were $R(F)/R_w$ ($I > 2\sigma_I$) = 3.2/3.7% with the largest residual in the ΔF map, 1.69 $e^-/Å^3$, located 0.86 Å from K2.

Table 1. Selected Data Collection and Structural Refinement Parameters for $K_5As_3Pb_3$

fw	1041.86
crystal system, space group, Z	orthorhombic, *Pnma* (No. 62), 4
unit cell dimensions	
a, Å	19.451(6)
b, Å	12.164(3)
c, Å	6.581(1)
V, Å^3	1557.0(6)
calcd density, g cm^{-3}	4.444
abs coeff μ (Mo Kα, cm^{-1})	400.37
R, R_w [a]	0.032, 0.037

[a] $R = \sum||F_o| - |F_c||/\sum|F_o|$; $R_w = [\sum w(|F_o| - |F_c|)^2/\sum w(F_o)^2]^{1/2}$; $w = \sigma_F^{-2}$.

Table 2. Refined Atomic Positions for $K_5As_3Pb_3$

atom	Wyckoff	x	y	z	B_{eq} [a]
Pb1	8*d*	0.04435(5)	0.11826(7)	0.4794(1)	1.55(2)
Pb2	4*c*	0.19349(8)	1/4	0.4397(2)	1.80(3)
As1	4*c*	0.9567(2)	1/4	0.2410(5)	1.46(7)
As2	8*d*	0.1526(1)	0.0534(2)	0.2361(4)	1.51(5)
K1	4*a*	0.0	0.0	0.0	1.9(2)
K2	4*c*	0.1033(5)	1/4	0.950(1)	1.8(2)
K3	8*d*	0.1788(3)	0.9545(5)	0.7293(8)	2.3(1)
K4	4*c*	0.3685(6)	1/4	0.761(1)	3.5(2)

[a] $B_{eq} = {}^8/_3\pi^2(U_{11}(aa^*)^2 + U_{22}(bb^*)^2 + U_{33}(cc^*)^2)$.

Table 3. Atom Separations (Å) in $K_5As_3Pb_3$

atom pair	distance	atom pair	distance
Pb1−Pb1	3.205(2)	As1−K3 ×2	3.630(8)
Pb1−Pb1	3.366(2)	As1−K4	3.64(1)
Pb1−Pb2	3.324(2)	As1−K4	3.61(1)
Pb1−As1	2.817(4)	As2−K1	3.413(3)
Pb1−As2	3.761(3)	As2−K2	3.191(6)
Pb1−K1 ×2	3.573(1)	As2−K3	3.582(7)
Pb1−K2 ×2	3.671(7)	As2−K3	3.280(8)
Pb1−K3	3.676(7)	As2−K3	3.499(7)
Pb1−K4	3.98(1)	As2−K4	3.744(3)
Pb2−As2 ×2	2.854(3)	K1−K2 ×2	3.660(5)
Pb2−K2	3.789(8)	K1−K3 ×2	3.947(7)
Pb2−K2	3.668(8)	K1−K4 ×2	4.218(8)
Pb2−K3 ×2	3.778(7)	K2−K3 ×2	4.146(8)
Pb2−K3 ×2	4.078(6)	K2−K4	4.59(2)
Pb2−K4	4.18(1)	K3−K3 ×2	4.440(9)
As1−K1 ×2	3.532(2)	K3−K4	4.11(1)
As1−K2	3.44(1)	K3−K4	4.44(1)

Selected crystallographic and refinement data are given in Table 1, and more detailed information and displacement ellipsoid parameters are in the Supporting Information, Tables S1 and S2. Refined atom positions are listed in Table 2, and the bond distances are in Table 3.

Theoretical Calculation. These were made over 326 *k*-points in the irreducible wedge with the aid of the CAESAR EHTB program of Whangbo et al.[15] Only the lead and arsenic atoms were included (H_{ii} and ζ_1 for Pb 6s, −15.70 eV and 2.35; for Pb 6p, −8.00 eV and 2.06; for As 5s, −12.60 and 2.23; and for As 5p, −6.190 and 1.89[16]). Calculations were carried out both for the isolated cluster $As_3Pb_3^{5-}$ and for the full anion structure in the unit cell.

(9) (a) Eisenmann, B.; Cordier, G. In *Chemistry, Structure and Bonding in Zintl Phases and Ions*; Kauzlarich, S. M., Ed.; VCH Publishers: New York, 1996; Chapter 2. (b) Schäfer, H.; Eisenmann, B. *Rev. Inorg. Chem.* **1981**, *3*, 29.

(10) Corbett, J. D. In *Chemistry, Structure and Bonding in Zintl Phases and Ions*; Kauzlarich, S., Ed.; VCH Publishers: New York, 1996; Chapter 3.

(11) Corbett, J. D. *Angew Chem., Int. Ed.* **2000**, *39*, 671.

(12) Dong, Z.-C.; Corbett, J. D. *J. Am. Chem. Soc.* **1993**, *115*, 11299.

(13) Klem, M. T.; Vaughey, J. T.; Harp, J. G.; Corbett, J. D. *Inorg. Chem.* **2001**, *40*, 7020.

(14) TEXSAN, Windows version 1.02; Molecular Structure Corp.: The Woodlands, TX, 1997.

(15) Ren, J.; Liang, W.; Whangbo, M.-H. *CAESAR*; PrimeColor Software, Inc.: Raleigh, NC, 1998.

(16) Alvarez, A. *Tables of Parameters for Extended Hückel Calculations*; Barcelona, Spain, 1987.

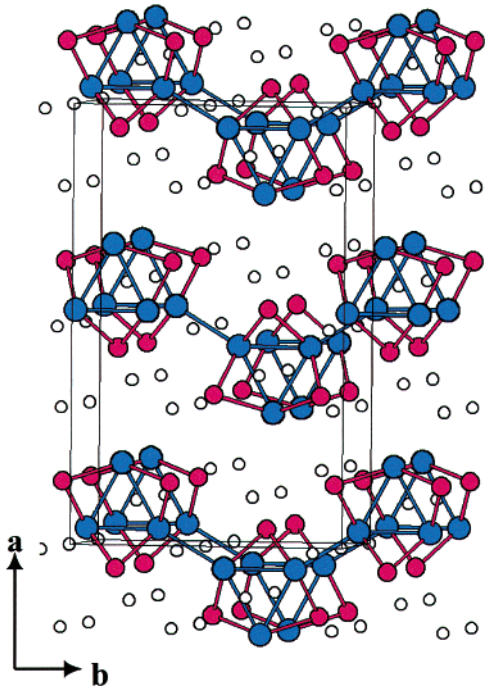

Figure 1. [001] view of the structure of $K_5Pb_3As_3$ with Pb, blue; As, red; and K, white.

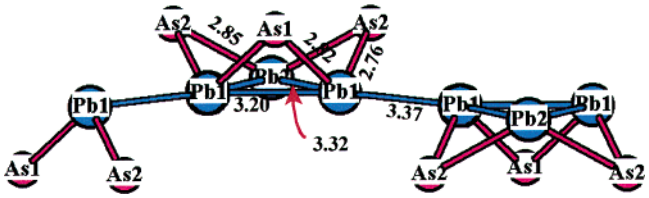

Figure 2. Detail of the $Pb_3As_3^{5-}$ anion and the intercluster linkages. A vertical mirror plane passes through Pb2 and As1.

Property Measurements. Resistivities of $K_5As_3Pb_3$ were measured by the electrodeless Q method[17] on 43.6 mg of powder that had been sieved to 250−425 μm and diluted with chromatographic Al_2O_3. Measurements were made at 34 MHz over 120−240 K. The resistivity of $K_5As_3Pb_3$ extrapolated to 298 K was 1.0×10^2 $\mu\Omega\cdot$cm with a temperature coefficient $[(\delta\rho/\delta T)/\rho]$ of $-0.14(3)$ K^{-1}. The temperature dependencies are quite reproducible by this method; on the other hand, the absolute resistivities may be off by a factor of 2 or 3.

Results and Discussion

Structure Description. The basic structural unit consists of somewhat flattened As_3Pb_3 "crown" clusters that are linked via intercluster Pb1−Pb1 bonds into chains that propagate along the *b* axis, Figure 1. The base of the crowns is defined by a triangle of Pb atoms with As atoms that bridge Pb−Pb edges as the points of a crown. The cluster possesses C_s symmetry with the vertical mirror planes through As1 and Pb2 and perpendicular to the page, but it is close to an ideal C_{3v} assignment, Figure 2. The edges of the base are 3.205(2) Å (Pb1−Pb1) and 3.324(2) Å (×2) (Pb1−Pb2). The shorter Pb1−Pb1 edge is bridged by an As1 atom with d(Pb1−As1) = 2.817(4) Å, and the other two Pb1−Pb2 edges by As2 atoms at distances of 2.761(3) Å and 2.854(3) Å to the neighboring Pb1 and Pb2 atoms, respectively. Finally, the resulting crowns are linked via longer Pb1−Pb1 intercluster bonds (3.366(2) Å) to generate chains of As_3Pb_3 clusters along the $\vec{b}$ direction, Figure 2. The exo Pb1−Pb1 bonds lie on centers of symmetry so the crown orientations alternate along the chains. It is noteworthy that the shortest intracluster bond is associated with five-bonded Pb1. The chains are well separated from one another with a minimum distance of 5.14 Å.

The cations serve their expected roles and bridge edges and cap faces about the As_3Pb_3 crown clusters. The K1 cations cap the triangular faces defined by the three cluster As atoms, K2 caps faces of two As and one Pb atom on two separate chains, K3 bridges pairs of As2 atoms on two As_3Pb_3 clusters, and K4 sits in a void defined by four As_3Pb_3 clusters (three within a chain and one above).

Some similarities exist between the $[As_3Pb_3]^{5-}$ motif in the present phase and the one found in $Cs_5In_3As_4$.[18] The indium phase contains both chains and layers with the same overall composition of $[In_3As_4]^{5-}$. The latter units are quite similar in appearance to that here except that a fourth As atom caps the open In_3 face opposite the As crown points, the clusters are interconnected by pairs of In−As bonds, and the dimers are interconnected by two longer In−In bonds. The two cluster skeletons are isoelectronic, the indium ⟹ lead conversion compensating for the three valence electrons of the fourth arsenic.

Bonding. The electronic requirements for the ideal isolated $As_3Pb_3^{5-}$ cluster can be deduced from Wade's empirical rules. The $As_3Pb_3^{5-}$ crowns would correspond to a *hypho*-cluster, with three basal lead vertices removed from the closo D_{3h} parent of a tricapped trigonal prism Pb_6As_3, although there remains a question as to whether such rules would apply when adjacent vertices are removed. According to Wade's rules, the number of skeletal p electrons required for closed shell bonding of a *hypho*-cluster would be $2n + 8$ or 20 skeletal electrons in this case. These come from three lead atoms (6), three arsenic atoms (9), and electrons from the five cations (5). Molecular orbital calculations support this treatment of an isolated cluster.

Complications arise when one takes into consideration the two intercluster Pb−Pb bonds formed by each $As_3Pb_3^{5-}$ cluster. Each exo bond should lower the electron requirements of each cluster by one, which leaves the compound with two excess electrons per cluster that need to be accounted for. Direct EHTB calculations were therefore carried out on the full anion structure in one cell. The resulting DOS and COOP curves shown in Figure 3 reflect a fairly localized bonding situation. The former densities-of-states plot shows that a small band gap opens just above the Fermi level (dashed line). This gap, it is hypothesized, should increase when K bonding/antibonding states mix in. The As s contributions (dotted) start below −20 eV and continue up to approximately −14 eV, and the lower lying Pb s (blue) behaves similarly. There is clearly a substantial amount of mixing between the As s and Pb s orbitals. The

(17) Zhao, J.-T.; Corbett, J. D. *Inorg. Chem.* **1995**, *34*, 378.

(18) Gascoin, F.; Sevov, S. C. *Inorg. Chem.* **2001**, *40*, 6254.

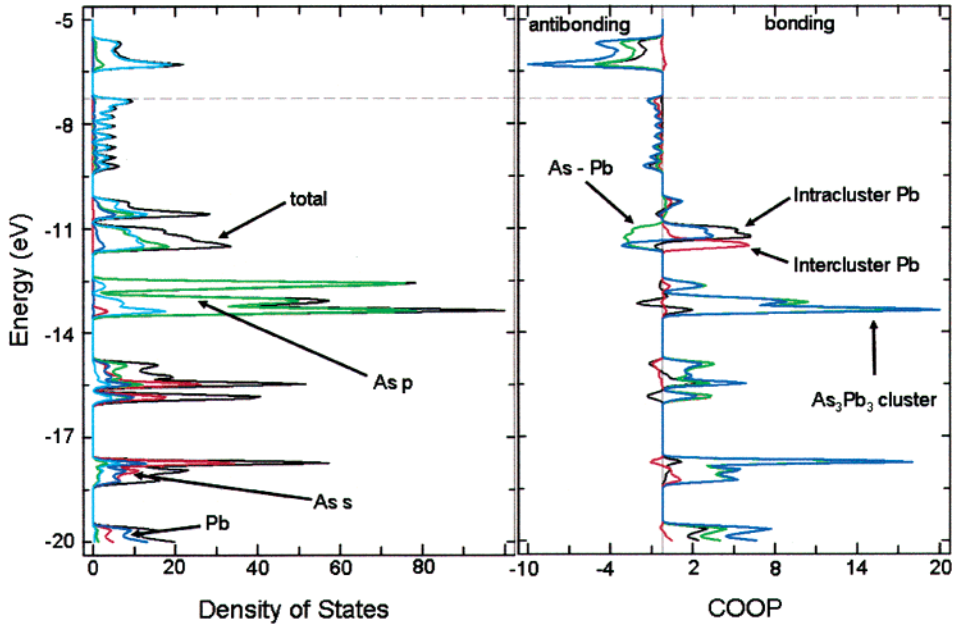

Figure 3. DOS and COOP data for the full anion structure of $K_5Pb_3As_3$. DOS, total and projected contributions: total, black; As s, red, Pb s,p, blue; As p, green. COOP: As_3Pb_3 cluster, blue; As−Pb, green; intracluster Pb, black; intercluster Pb, red.

As p contributions (green) begin around −15 eV and continue up to −10 eV, and the Pb p portion (also blue) starts around −13 eV and continues to past E_F. The As p orbitals dominate from −13 eV to −10 eV, at which point the Pb p gains dominance. There is a good amount of mixing between the As p and Pb p up to about −8 eV, above which point Pb p is dominant. The arsenic contributions are narrower because they function only as terminal atoms whereas the lower lying lead AOs are broadened appreciably because of the multicentered bonding of lead.

The COOP curve for the $As_3Pb_3^{5-}$ cluster (blue) shows that weakly antibonding states are populated just below the Fermi energy, predominantly As−Pb and Pb1−Pb1 intercluster π states (green). There appear to be few contributions from antibonding states on the intercluster Pb_3 triangle at Fermi (red). Interestingly, the ideal $As_3Pb_3^{5-}$ cluster chain bonding (blue), which corresponds to 18 skeletal electrons per $As_3Pb_3^{5-}$ cluster, would be optimized at approximately −9.5 eV. This is in agreement with the prediction afforded by Wade's rules for the 6-atom *hypho*-cluster with two exo bonds. Added occupancy of the π^* states by the "extra" two electrons has only small antibonding effects.

The effect of populating the additional intracluster antibonding states is evident in the overlap populations. The overlap population for the intercluster Pb1−Pb1 contacts at 3.37 Å is 0.37, whereas that for the average intracluster Pb−Pb contacts, 3.26 Å, is 0.20; i.e., the former is 85% larger in overlap population with a 0.1 Å *longer* bond relative to the average intracluster Pb−Pb. Since the intercluster antibonding states are not being populated, this is not surprising. The average overlap population for As−Pb bonds also remains relatively high, 0.47. Thus, extended Hückel bonding analysis suggests that this phase has a good prospect of being a valence compound and exhibiting semiconducting behavior. The measured microwave resistivity for $K_5As_3Pb_3$ supports this assessment, being 1.03×10^2 $\mu\Omega$·cm at room temperature with a negative temperature coefficient of -0.14 K^{-1}. These data are given in the Supporting Information.

The isolated $As_3Pb_3^{5-}$ cluster represents a new type of hyperelectronic Zintl cluster with a heavy tetrel framework capped by arsenic. It also represents an expansion of the known heteroatomic Zintl clusters of the tetrel elements in a new direction, and an alternative to the less reasonable large clusters associated with relatively few cations for classic closo species. The ability to rationalize the cluster geometry with the observed excess electron count enables one to make this assignment. Even though the compound is infinitely bonded through intercluster bonding, the extra electrons evidently remain localized on the individual clusters. The driving force for the higher cluster charges here must be 2-fold: first, the accommodation of extra cations increases the Madelung energy and helps separate the anion chains, and second, the extra electrons are bound in only weakly antibonding and fairly localized states. This is a novel alternative to the usual result for hyperelectronic "Zintl" phases with extra cations in which the added electrons are delocalized, again in a presumably low lying but open band. The clearest example of the latter presently is the metallic Na_6TlSb_4 in which extra electrons are accommodated in Na−Sbπ bands.[19,20]

Supporting Information Available: Tables of crystal and refinement data and anisotropic displacement parameters; figure of resistivity data all for $K_3Pb_3As_3$. This material is available free of charge via the Internet at http://pubs.acs.org.

IC040045R

(19) Li, B.; Chi, L.; Corbett, J. D. *Inorg. Chem.* **2003**, *42*, 3036.
(20) Mudring, A.-V.; Corbett, J. D. *Z. Anorg. Allg. Chem.*, submitted.